Nature Environment and Pollution Technology
An International Quarterly Scientific Journal

p-ISSN: 0972-6268
e-ISSN: 2395-3454

Vol. 19 | No. 1 | pp. 389-393 | 2020

Original Research Paper | Open Access

The Removal of Phosphorus in Solution by the Magnesium Modified Biochar from Bamboo

Jing Dai*, Xitong Zheng*, Hong Wang, Hao Zhang**, Linli Zhang, Tianbiao Lin, Rui Qin* and Muqing Qiu*†**
*College of Life Science, Shaoxing University, Shaoxing, 312000, P.R. China
**Key Laboratory of Agro-Ecological Processes in Subtropical Region, Institute of Subtropical Agriculture, Chinese Academy of Sciences, Changsha 410125, China
†Corresponding author: Muqing Qiu

Nat. Env. & Poll. Tech.
Website: www.neptjournal.com

Received: 14-06-2019
Accepted: 24-07-2019

Key Words:
Phosphorus
Magnesium modified biochar
Bamboo

ABSTRACT

The eutrophication of water would cause the quality of the water to deteriorate and the algae to grow in large quantities. The recovery of phosphorus from sewage can not only purify the water quality, but also achieve the recycling of phosphorus. Its environmental and economic benefits are considerable. In this study, bamboo was used as raw material and modified with MgCl2 solution to prepare Mg-loaded biochar from bamboo (Mg@B). The adsorption experiments of phosphorus in solution by Mg@B were carried out. The adsorption kinetics of phosphorus by Mg@B was depicted by pseudo-first order kinetic and pseudo-second order kinetic models. The results showed that the surface of Mg@B is covered with the compound of Mg(OH)2. The adsorption process fits well with the pseudo-second order kinetics equation. The predominant process is chemisorption, which involves a sharing of electrons between the adsorbate and the surface of the adsorbent. The factor limiting the rate of reaction is primarily the number of surface-active sites of the adsorbent. The mechanism of Mg@B adsorbing phosphate ions in solution has physical adsorption, electrostatic adsorption and chemical precipitation.

INTRODUCTION

With the rapid development of industry and agriculture, the emissions of eutrophic substances, such as N, P, and so on, have also increased dramatically. The eutrophication of water would cause the water quality of the water to deteriorate and the algae to grow in large quantities (Jiang et al. 2019, Pinto et al. 2019). For a long time, in order to control the eutrophication of water bodies, many scholars have carried out related scientific research work, such as A/O, A/A/O, UASB and so on (Shamim & Joann 2016, Elsa et al. 2018, Khouloud et al. 2018, Zhang et al. 2018). These wastewater treatment methods are effective in treatment of phosphorus in solution, and the effect is better. As a non-renewable resource, phosphorus is a kind of the indispensable resource in agricultural development. The recovery of phosphorus from sewage can not only purify the water quality, but also achieve the recycling of phosphorus. Its environmental and economic benefits are considerable (Sarah et al. 2018, Sun et al. 2018). At present, the development direction of phosphorus treatment technology has shifted from removal of phosphorus in solution to recovery of phosphorus in wastewater (Fang et al. 2015). The treatment methods used for phosphorus recovery mainly include chemical precipitation, crystallization, ion exchange, adsorption, and so on (He et al. 2014, Huang et al. 2018, Qiu et al. 2018, Sanna et al. 2018). The adsorption method is applied widely because of its simple operation, no secondary pollution, and low price. The most commonly used adsorbents are activated carbon, modified cellulose, etc., but these adsorbents are limited in their application due to their high cost (Jessica et al. 2017). Therefore, some researchers have begun to use low-cost agricultural waste to prepare biochar, such as bamboo, peanut shell, tangerine skin, corn straw, rice straw, sawdust, reeds, and so on (Gottipati & Mishra 2013, Xu et al. 2014, Hu et al. 2017, Sarah et al. 2018). However, the surface of the prepared biochar contains a large amount of negative charge (Yigit & Mazlum 2007). These negative charges are very easy to generate electrostatic repulsion with anions, so it is difficult to adsorb PO_4^{3-} ions in solution. In order to improve their adsorption capacity of anions, many scholars apply acid, alkali, iron oxide, magnesium ion, rare earth and so on to modify the surface of these biochars (Stratful et al. 2001, Tansel et al. 2018).

In this study, bamboo was used as raw material and modified with $MgCl_2$ solution to prepare Mg-loaded biochar from bamboo (Mg@B). The adsorption experiments of phosphorus in solution by Mg@B were carried out. The adsorption kinetics of phosphorus by Mg@B was depicted by pseudo-first order kinetic and pseudo-second order kinetic models. The adsorption characteristics of phosphorus in

solution were studied by scanning electron microscope (SEM), Fourier infrared spectroscopy (FTIR) and X-ray diffraction spectrum (XRD) techniques. The adsorption mechanisms have also been discussed.

MATERIALS AND METHODS

Preparation of Mg@B

The biochar from bamboo is ground and passed through a 100 meshes sieve. Its specific surface area is 60.125 m^2/g, and average pore size is 10. 2.109 nm. The 10 g biochar from bamboo was added to the 500 mL Erlenmeyer flasks containing 100 mL 2 mol/L $MgCl_2$ solution. Then, 100 mL 4.5 mg/L NaOH was added slowly. They were shaken in an ultrasonic shaker for 60 minutes. The mixture solution was filtered through a qualitative filter paper. The precipitate was washed three times with the deionized water. The precipitate was dried at 60°C for 48 hours in an oven and calcined at 450°C for 2 hours in a muffle furnace to obtain the Mg-loaded biochar from bamboo (Mg@B).

Characterization of Mg@B

The morphology of Mg@B was observed with SEM (JEOL 6500F, Japan). The XRD analysis was conducted in a D/Max-IIIA powder X-ray diffraction spectrum (Rigaku Corp., Japan). FTIR spectra of the samples were recorded on a Nexus 670 FTIR spectrometer (Thermo Nicolet, Madison) in the wave number range of 500-4000 cm^{-1}.

Adsorption Experiment

Adsorption experiments were conducted in a set of 250 mL Erlenmeyer flasks containing 0.02 g Mg@B and 100 mL of 50 mg/L PO_4^{3-} ion solutions. The initial pH was adjusted to 4.0 with 1 mol/L HCl. The flasks were placed in a shaker at a constant temperature of 298 K and 200 rpm. The samples were filtered and analysed.

Analytical Methods

The concentration of PO_4^{3-} ion was analysed by UV-722 UV-visible spectrophotometry. The removal rate of PO_4^{3-} ion was calculated as follows:

$$Q = \frac{C_0 - C_t}{C_0} \times 100\% \quad \ldots(1)$$

Where, C_0 and C_t (mg/L) are the initial and equilibrium concentrations of PO_4^{3-} ion in solution respectively. Q is the removal rate of PO_4^{3-} ion.

Statistical Analyses of Data

All the experiments were repeated in duplicate and the data of results were the mean and the standard deviation (SD). The value of the SD was calculated by Excel software. All the error estimates given in the text and error bars in figures are standard deviation of means (mean ± SD). All the statistical significance was noted at $\alpha = 0.05$ unless otherwise noted.

RESULTS AND DISCUSSION

Characterization of Mg@B

The morphology of biochar and Mg@B were observed with SEM. The results are shown in Fig. 1.

From Fig. 1, it can be seen that biochar from bamboo is a porous material. After modification of magnesium, the surface of biochar is covered with a thick layer of flocculent material. This flocculent substance should be a compound of magnesium. The magnesium compound is uniformly

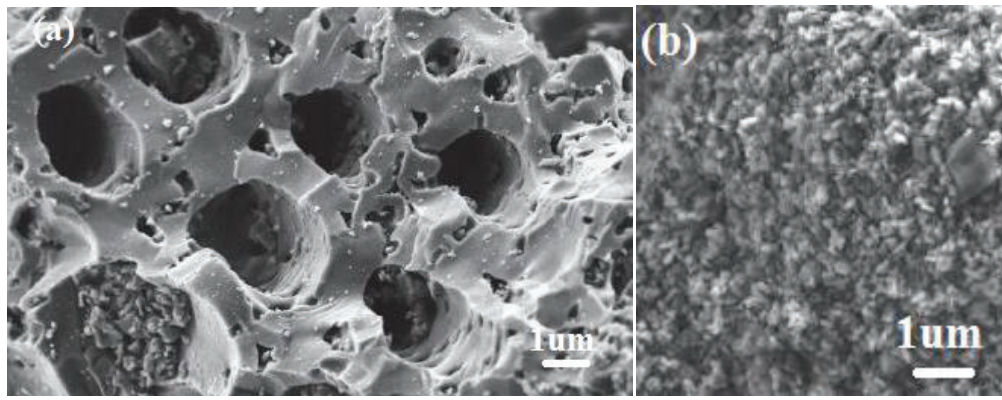

Fig. 1: The SEM images of biochar and Mg@B (a, biochar; b, Mg@B).

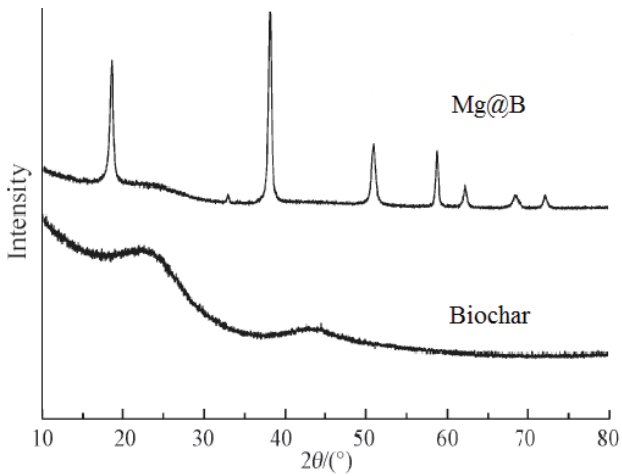

Fig. 2: The XRD spectra of biochar and Mg@B.

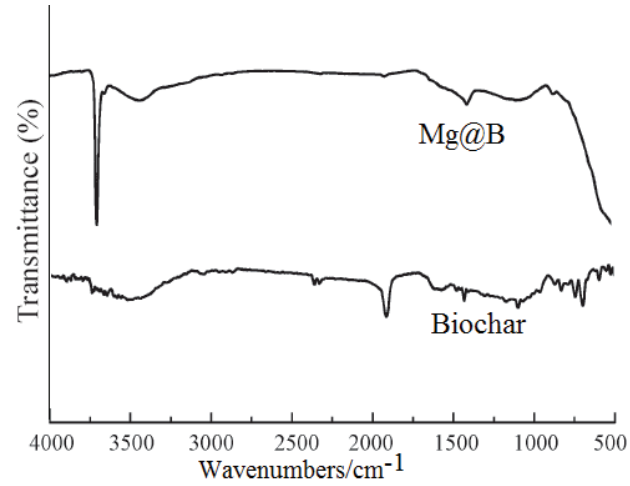

Fig. 3: FTIR spectra of biochar and Mg@B.

supported on the surface of the biochar and inside the pore diameter.

The XRD analysis of biochar and Mg@B were conducted in a D/Max-IIIA Powder X-ray diffraction spectrum. The results are shown in Fig. 2.

As shown in Fig. 2, it can be concluded that after modification of magnesium, many high-intensity diffraction peaks of $Mg(OH)_2$ appeared. It also indicates that the modified magnesium has been successfully loaded on the biochar from bamboo. It can also be shown in FTIR spectra of Mg@B (Fig. 3). There is a distinct characteristic absorption peak of $Mg(OH)_2$ at a wavelength of 3694.2 cm^{-1}.

Adsorption Experiment

The effect of adsorption time on the PO_4^{3-} ion removal rate by Mg@B is shown in Fig. 4.

As shown in Fig. 4, it can be seen that the removal rate of PO_4^{3-} ion in solution by Mg@B increased rapidly within 30 minutes. At 60 minutes, the amount of PO_4^{3-} ion adsorbed is near saturation. After 240 minutes, the adsorption process reached equilibrium. The removal rate of PO_4^{3-} ion by Mg@B was reached 64.12%.

Adsorption Kinetics

In this study, the pseudo-first order and pseudo-second order were chosen to depict the adsorption kinetics. The pseudo-first order (Choudhary & Paul 2018) and pseudo-second order (Reguyal et al. 2017) reactions were described as Eqs. (1) and (2):

$$\frac{dq_t}{dt} = k_1(q_e - q_t) \quad \ldots(1)$$

$$\frac{dq_t}{dt} = k_2\left(q_e - q_t\right)^2 \quad \ldots(2)$$

Where, q_e (mg/g) is the amount of adsorbed solute at equilibrium conditions, q_t (mg/g) is the amount of adsorbed solute at any time t (min), k_2 (min^{-1}) and k_1 (min^{-1}) are the constants of pseudo-second order and pseudo-first order kinetic models respectively.

According to the experimental data from Fig. 4 and Equations (1) and (2), the corresponding calculated parameters are listed in Table 1.

From Table 1, it can be shown that the adsorption process fits well with the pseudo-second order kinetics equation according to the value of R^2 (0.9917). It implies that the predominant process is chemisorption, which involves a sharing of electrons between the adsorbate and the surface of the adsorbent. The factor limiting the rate of reaction is primarily the number of surface active sites of the adsorbent.

Adsorption Mechanism

The mechanism of biochar adsorbing phosphate ions is that phosphate ions can be bonded to certain metal cations in biochar by electrostatic adsorption or ligand bonding (Mukherjee & Zimmerman 2013). After the biochar is modified with magnesium, the following reaction would occur between the biochar and the phosphate ions in solution.

$$Biochar - Mg(OH)_2 + PO_4^{3-} + 6H_2O \rightarrow Biochar - Mg_3(PO_4)_2 \cdot 6H_2O \downarrow \quad \ldots(3)$$

In brief, the mechanism of Mg@B adsorbing phosphate ions in solution has physical adsorption, electrostatic adsorption and chemical precipitation.

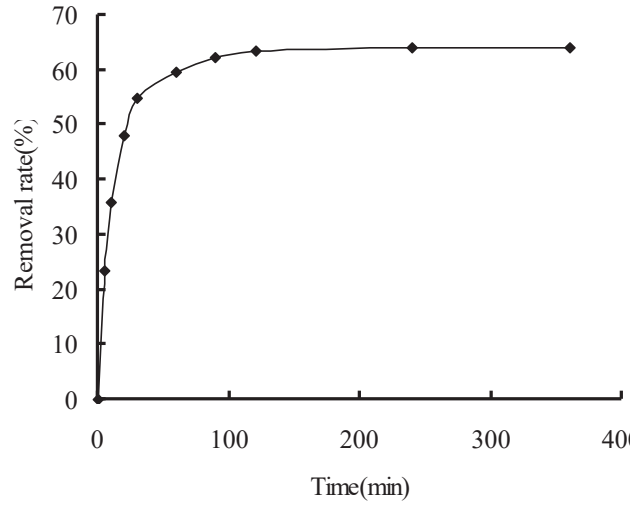

Fig. 4: Effect of adsorption time on the PO_4^{3-} ion removal rate by Mg@B.

Table 1: Pseudo-first order kinetic and pseudo-second order kinetic parameters of PO_4^{3-} ions removal by Mg@B.

Pseudo-first order			Pseudo-second order		
q_e (mg/g)	k_α (min^{-1})	R^2	q_e (mg/g)	k_β ($g/mg^{-1}/min^{-1}$)	R^2
125.17	0.0853	0.9241	130.25	0.001	0.9917

CONCLUSIONS

1. The surface of Mg@B is covered with a thick layer of flocculent material. This flocculent substance should be a compound of magnesium. According to the results of XRD spectrum and FTIR spectrum, the compound of magnesium on the surface of Mg@B is $Mg(OH)_2$.
2. The adsorption process fits well with the pseudo-second order kinetics equation. The predominant process is chemisorption, which involves sharing of electrons between the adsorbate and the surface of the adsorbent. The factor limiting the rate of reaction is primarily the number of surface active sites of the adsorbent.
3. The mechanism of Mg@B adsorbing phosphate ions in solution has physical adsorption, electrostatic adsorption and chemical precipitation.

ACKNOWLEDGEMENTS

This study was financially supported by the project of science and technology plan in Zhejiang Province (LGF19C030001), Guangxi Key Research and Development Program (AB17129002 and AB18050018)) and the project of science and technology plan in Shaoxing City (2017B70058).

REFERENCES

Choudhary, B. and Paul, D. 2018. Isotherms, kinetics and thermodynamics of hexavalent chromium removal using biochar. J. Environ. Chem. Eng., 6: 2335-2343.

Elsa, A., Mohan, V.J., Graham, B. and Philip, A.S. 2018. Isotherms, kinetics and mechanism analysis of phosphorus recovery from aqueous solution by calcium-rich biochar produced from biosolids via microwave pyrolysis. J. Environ. Chem. Eng., 6: 395-403.

Fang, C., Zhang, T., Li, P., Jiang, R.F., Wu, S.B., Nie, H.Y. and Wang, Y.C. 2015. Phosphorus recovery from biogas fermentation liquid by Ca-Mg loaded biochar. J. Environ. Sci., 29: 106-114.

Gottipati, R. and Mishra, S. 2013. Preparation of microporous activated carbon from Aegle marmelos fruit shell by KOH activation. Canadian J. Chem. Eng., 91: 1215-1222.

He, H., Qian, T.T., Liu, W.J., Jiang, H. and Yu, H.Q. 2014. Biological and chemical phosphorus solubilization from pyrolytical biochar in aqueous solution. Chemosphere, 113: 175-181.

Hu, B.W., Qiu, M.Q., Hu, Q.Y., Sun Y.B., Sheng, G.D., Hu, J. and Ma, J.Y. 2017. Decontamination of Sr(II) on magnetic polyaniline/graphene oxide composites: Evidence from experimental, spectroscopic, and modeling investigation. ACS Sustain. Chem. & Eng., 5: 6924-6931.

Huang, D.L., Deng, R., Wan, J., Zeng, G.M., Xue, W.J., Wen, X.F., Zhou, C.Y., Hu, L., Liu, X.G., Xu, P., Guo, X.Y. and Ren X.Y. 2018. Remediation of lead-contaminated sediment by biochar-supported nano-chlorapatite: Accompanied with the change of available phosphorus and organic matters. J. Hazard. Mater., 348: 109-116.

Jessica, G.S., Wolfram, B., Saran, P.S. and Kate, V.H. 2017. Bioavailability of phosphorus, other nutrients and potentially toxic elements from marginal biomass-derived biochar assessed in barley (*Hordeum vulgare*)

growth experiments. Sci. Total Environ., 584-585: 448-457.

Jiang, Y.H., Li, A.Y., Deng, H., Ye, C.H., Wu, Y.Q., Linmu, Y.D. and Hang, H.L. 2019. Characteristics of nitrogen and phosphorus adsorption by Mg-loaded biochar from different feedstocks. Bioresource Technol., 276: 183-189.

Khouloud, H., Salah, J., Mejdi, J., Aida, B.H.T. and Lionel, L. 2018. Investigations on phosphorus recovery from aqueous solutions by biochars derived from magnesium-pretreated cypress sawdust. J. Environ. Manag., 216: 305-314.

Mukherjee, A. and Zimmerman, A.R. 2013. Organic carbon and nutrient release from a range of laboratory-produced biochars and biochar-soil mixtures. Geoderma, 193: 122-130.

Pinto, M.C.E., Silva, D.D., Gomes, A.L.A., Santos, R.M.M., Couto, R.A.A., Novais, R.F., Constantino, V.R.L., Tronto, J. and Pinto, F.G. 2019. Biochar from carrot residues chemically modified with magnesium for removing phosphorus from aqueous solution. J. Clean. Prod., 222: 36-46.

Qiu, M.Q., Wang, M., Zhao, Q.Z., Hu, B.W. and Zhu, Y.L. 2018. XANES and EXAFS investigation of uranium incorporation on nZVI in the presence of phosphate. Chemosphere, 201: 764-771.

Reguyal, F., Sarmah, A.K. and Gao, W. 2017. Synthesis of magnetic biochar from pine sawdust via oxidative hydrolysis of $FeCl_2$ for the removal off sulfamethoxazole from aqueous solution. J. Hazard Mater., 321: 868-878.

Sanna, S., Mari, R., Maarit, H. and Perttu, V. 2018. Biochar addition changed the nutrient content and runoff water quality from the top layer of a grass field during simulated snowmelt. Agr. Ecosyst. Environ., 265: 156-165.

Sarah, V.N., Mariana, D.O.Z., Jairo, T., Rafaela, F.C. and Carlos, E.P.C. 2018. Poultry manure and sugarcane straw biochars modified with $MgCl_2$ for phosphorus adsorption. J. Environ. Manag., 214: 36-44.

Sarah, V.N., Mariana, D.O.Z., Matheus, S.C.B., Célia, R.M. and Carlos, E.P.C. 2018. Phosphorus removal from eutrophic water using modified biochar. Sci. Total Environ., 633: 825-835.

Shamim, G. and Joann, K.W. 2016. Biochemical cycling of nitrogen and phosphorus in biochar-amended soils. Soil Biol. Biochem., 103: 1-15.

Stratful, I., Scrimshaw, M.D. and Lester, J.N. 2001. Conditions influencing the precipitation of magnesium ammonium phosphate. Water Res., 35: 4191-4199.

Sun, D.Q., Hale, L., Kar, G., Soolanayakanahally, R. and Adl, S. 2018. Phosphorus recovery and reuse by pyrolysis: Applications for agriculture and environment. Chemosphere, 194: 682-691.

Tansel, B., Lunn, G. and Monje, O. 2018. Struvite formation and decomposition characteristics for ammonia and phosphorous recovery: A review of magnesium-ammonia-phosphate interaction. Chemosphere, 194: 504-512.

Xu, G., Sun, J.N., Shao, H.B. and Chang, S.X. 2014. Biochar had effects on phosphorus sorption and desorption in three soils with differing acidity. Ecol. Eng., 62: 54-60.

Yigit, N.O. and Mazlum, S. 2007. Phosphate recovery potential from wastewater by chemical precipitation at batch conditions. Environ. Technol. Lett., 28: 83-93.

Zhang, T., Xu, H.Y., Li, H.H., He, X.Y., Shi, Y.J. and Kruse, A. 2018. Microwave digestion-assisted HFO/biochar adsorption to recover phosphorus from swine manure. Sci. Total Environ., 621: 1512-1526.